

TIDAL BREAK-UP OF BINARY STARS AT THE GALACTIC CENTER AND ITS CONSEQUENCES

FABIO ANTONINI

Department of Physics and Center for Computational Relativity and Gravitation, Rochester Institute of Technology, 85 Lomb Memorial Drive, Rochester, NY 14623, USA

JOSHUA FABER

Center for Computational Relativity and Gravitation, School of Mathematical Sciences, Rochester Institute of Technology, 85 Lomb Memorial Drive, Rochester, NY 14623, USA

ALESSIA GUALANDRIS AND DAVID MERRITT

Department of Physics and Center for Computational Relativity and Gravitation, Rochester Institute of Technology, 85 Lomb Memorial Drive, Rochester, NY 14623, USA

Draft version October 29, 2018

ABSTRACT

The tidal breakup of binary star systems by the supermassive black hole (SMBH) in the center of the galaxy has been suggested as the source of both the observed sample of hypervelocity stars (HVSs) in the halo of the Galaxy and the S-stars that remain in tight orbits around Sgr A*. Here, we use a post-Newtonian N-body code to study the dynamics of main-sequence binaries on highly elliptical bound orbits whose periapses lie close to the SMBH, determining the properties of ejected and bound stars as well as collision products. Unlike previous studies, we follow binaries that remain bound for several revolutions around the SMBH, finding that in the case of relatively large periapses and highly inclined binaries the Kozai resonance can lead to large periodic oscillations in the internal binary eccentricity and inclination. Collisions and mergers of the binary elements are found to increase significantly for multiple orbits around the SMBH, while HVSs are primarily produced during a binary's first passage. This process can lead to stellar coalescence and eventually serve as an important source of young stars at the Galactic center.

Subject headings: black hole physics-Galaxy:center-Galaxy:kinematics and dynamics-stellar dynamics

1. INTRODUCTION

The center of the Milky Way can be regarded as a rather unusual galactic nucleus in many respects. The supermassive black hole (SMBH) at the Galactic center has a mass of $M_{\text{MW}} \sim 4 \times 10^6 M_{\odot}$ (Ghez et al. 2008; Gillessen et al. 2009), making it perhaps the smallest SMBH with a well-determined mass (Ferrarese & Ford 2005). Furthermore, while most known galactic nuclei have relaxation times much longer than the Hubble time, the relatively high density at the center of the Milky Way ($\gtrsim 10^6 \text{ stars pc}^{-3}$) and the small mass of the SMBH imply a two-body relaxation time that is as short as a few Gyr inside the SMBH influence radius (Alexander 2005). The combination of high stellar densities, large velocities, and short relaxation time effectively make the inner parsec of the Milky Way a collisional system.

In a collisional environment, otherwise rare dynamical processes can take place at an appreciable rate. These include dynamical encounters between stars, binaries and higher-order systems. If a massive black hole is present, as is believed to be the case for most, if not all, galactic nuclei, stars and binaries can interact with it and be ejected with extreme velocities. Gravitational encounters involving stellar binaries and the SMBH have recently been studied by several authors in the context of hypervelocity stars (HVSs) (Gualandris et al. 2005; Bromley et al. 2006;

Ginsburg & Loeb 2006; Sesana et al. 2007). HVSs have such extreme velocities ($500 - 1000 \text{ km s}^{-1}$ as measured in the Galactic halo) that they require a dynamical encounter with a massive black hole for their explanation (Hills 1988; Yu & Tremaine 2003). The idea is that stellar binaries on low angular momentum orbits interact with the SMBH and are dissociated by its strong tidal field. As a result, one component is captured by the SMBH into a wide eccentric orbit while the other star is ejected to infinity with large velocity. After the fortunate discovery of the first HVS in the Galactic halo (Brown et al. 2005), a handful have been found escaping the Galaxy at large speeds (Brown et al. 2006). More recent surveys of hypervelocity stars found 16 stars with velocities larger than the Galactic escape velocity (Brown et al. 2007, 2009).

Given the high stellar density at the Galactic center, it is plausible that stars interacting with the SMBH will come close enough to each other that finite size effects become important and physical collisions occur. In this case, the SMBH acts as catalyst for their interaction. Ginsburg & Loeb (2007) (hereafter GL07) first noted that the tidal breakup of a stellar binary interacting with the SMBH can lead, at least for some orbital parameters, to a physical collision soon afterwards. If the two stars collide with a relative impact speed smaller than the escape speed from their surface, coalescence can occur, resulting in the formation of a new, heavier star.

Using Aarseth's direct integration scheme (Aarseth

1999) to investigate the dynamics of the encounter, Ginsburg & Loeb found that the rate of collision events at the Galactic center is about ten times smaller than the rate of formation of hypervelocity stars ($\sim 10^{-5}\text{yr}^{-1}$, Brown et al. 2006), and that among the collision products, stellar coalescence occurs in about twenty percent of the cases. In this paper we expand on their work and investigate the possibility that stellar encounters with the SMBH are responsible for the production of a population of rejuvenated stars around the SMBH.

If a binary approaches the SMBH within its tidal disruption radius, at the periastron the stars can reach velocities a few percent of light speed, making relativistic effects potentially important in determining the properties of the unbound population and the rate at which the stars are ejected at hypervelocities. Here, we perform the first N -body simulations of binary-SMBH encounters that include post-Newtonian (PN) terms up to order 2.5, for both star-SMBH and star-star interactions.

In §2 and §3, we describe the parameters we chose for our N -body evolutions and their physical motivation. In §4, we discuss the likelihood of tidal capture of stars by the SMBH during close passages of binary systems. §5 and §6 consider in greater detail the populations of HVSs and stellar collision/merger products, respectively, including mechanisms like Kozai resonance that are critical in understanding the long-term evolution of binary systems. A systematic comparison between Newtonian and PN integrations is provided throughout. Finally, in §6, we provide a summary and discuss future avenues of study.

2. INITIAL MODELS AND NUMERICAL METHODS

We use N -body simulations to study the evolution of main sequence binaries as they make close passages by the SMBH at the Galactic center. We determine the conditions under which gravitational interactions produce HVSs, and the properties of the resulting distribution of both unbound and bound stars. All the simulations were carried out using the ARCHAIN (Mikkola & Merritt 2008) integrator, which includes PN corrections to all pairwise forces up to order PN2.5. The code employs an algorithmically regularized chain structure and the time-transformed leapfrog scheme to accurately trace the motion of tight binaries with arbitrarily large mass ratios (Mikkola & Aarseth 2002; Mikkola & Merritt 2006).

Given the significant computational resources per run made necessary by the high precision of our simulations we focus on a simplified set of initial conditions. We consider circular equal-mass binary systems with random initial orientations, initial separations $a_0 = 0.05\text{--}0.2\text{ AU}$, and individual stellar masses $M_* = 3\text{--}6 M_\odot$. We define M_b to be the total mass of the binary system. Obviously, the choice of equal-mass components limits our work. A treatment of binaries with a spectrum of masses similar for instance to that found in Duquennoy & Mayor (1991) is outside the scope of this paper, but could be included in a future work.

We give the binary a tangential initial velocity v_{in} at a distance $d = 0.01\text{--}0.1\text{ pc}$ from the SMBH of mass $M_\bullet = 4 \times 10^6 M_\odot$, in effect setting the periastron distance:

$$r_{\text{per}} = \frac{(v_{\text{in}}d)^2}{2GM_\bullet - v_{\text{in}}^2d} \quad (1)$$

for a Newtonian elliptical orbit.

Our initial binary separations are close to the extremes of the interval within which HVSs are produced. Since the ejection velocity increases with the internal binary energy, few stars will be ejected with velocities sufficiently large to escape from the Galaxy for $a_0 > 0.2\text{ AU}$, unless very large stellar masses are considered (Gualandris et al. 2005). We also note that, for the initial distances d we choose, binaries with $a_0 > 0.2\text{ AU}$ are unlikely to survive for many orbits around the SMBH due to close encounters with field stars (Perets 2009a). The lower limit of 0.05 AU is required by the consideration that smaller separations will result in contact binaries. GL07 pointed out that, assuming a constant probability per $\ln(a_0)$ for $0.02 < a_0 < 20\text{ AU}$, the probability to find a binary with a separation within the considered interval is $\sim 20\%$. We place the binaries on highly elliptical orbits about the SMBH, rather than e.g. on parabolic/hyperbolic orbits (Gould & Quillen 2003).

The origin of the young stars (and binaries) in the Galactic center is still a matter of ongoing research. One possibility is that stars/binaries formed in-situ, i.e. at distances of a few tens of milliparsecs from the SMBH. This model faces severe difficulties since tidal forces from the SMBH inhibit star formation at these distances. Instead, it is typically assumed that the stars need to form further away from the SMBH and then migrate to the center within their lifetimes. Among the various migration models that have been proposed, three produce orbits similar to those considered in this work (i.e. highly eccentric): (i) the eccentric disk instability scenario (Madigan et al. 2008) (ii) the cluster infall scenario aided by an intermediate mass black hole (IMBH) (Gerhard 2001) and (iii) the triple disruption scenario (Perets 2009b). The first model considers a dynamical instability of an eccentric disk as the mechanism that drives the eccentricities of the stars away from their initial values and produces near-radial orbits within a few Myr. The second model assumes stars and binaries form during the collapse of a giant molecular cloud and inspiral due to dynamical friction toward the Galactic center. The cluster, which is subject to tidal disruption, can reach distances of $10\text{--}50\text{ mpc}$ if it harbors an IMBH of mass $\gtrsim 10^3 M_\odot$ at its center. Tidally removed stars can then be scattered onto eccentric orbits by the IMBH (Merritt et al. 2009). Finally, in the triple disruption scenario, young and runaway stars can form by disruptions of triples by the SMBH, which in some cases results in the capture of binaries on close orbits.

At least some of the binary progenitors of observed HVSs were likely to have been part of the young stellar disk observed at the Galactic center, whose inner edge lies at a radius 0.1 pc from the SMBH (Löckmann et al. 2008), and this fact motivated our choice for the maximum value of d . The distance 0.01 pc adopted as a minimum value for d is comparable to the radii of the smallest observed stellar orbits at the Galactic center (Eckart & Genzel 1997; Genzel et al. 1997).

3. BASIC RELATIONS

Three radii play a fundamental role in our simulations:

- the periastron separation r_{per} of the initial orbit of the binary with respect to the SMBH;

- the tidal disruption radius r_t of a single star due to the SMBH;
- the tidal disruption (i.e. breakup) radius r_{bt} of the binary due to the SMBH.

A binary with initial separation a_0 will be broken apart by tidal forces if its center of mass approaches the massive object within the distance (Miller et al. 2005; Sesana et al. 2009)

$$r_{bt} \sim \left(3 \frac{M_\bullet}{M_b}\right)^{1/3} a_0. \quad (2)$$

As Hills (1988) noted, the tidal disruption of single stars is an important issue in the context of binaries. Because of their low densities, main sequence (MS) stars do not survive close interactions with the SMBH; small initial velocities take the stars too close to the SMBH and no HVSs are produced (compact objects, e.g., neutron stars and white dwarfs, can survive significantly closer approaches). Tidal disruption occurs for stars that approach the SMBH more closely than r_t , where

$$r_t \sim \left(\frac{M_\bullet}{M_*}\right)^{1/3} R_*, \quad (3)$$

with R_* the stellar radius. We assume a mass-radius relation $R_*/R_\odot = (M_*/M_\odot)^{0.75}$ (Hansen et al. 2004) which yields $R_* = 0.01$ AU for $M_* = 3 M_\odot$, and $R_* = 0.016$ AU for $M_* = 6 M_\odot$. Stars with orbits meeting the criterion $r_{\text{per}} < r_t$ are fully disrupted (Luminet & Carter 1986; Evans & Kochanek 1989; Faber et al. 2005). Note that this condition is stronger than the classical Roche limit formula given by Paczynski (1971) and Eggleton (1983). Even when tidal disruption does not occur, we expect that mass will be stripped from the outer regions of any star passing within the Roche limit, which would have a fundamental impact on the subsequent evolution and orbit of the stars.

For $M_* = 3 M_\odot$ and $M_\bullet = M_{\text{MW}}$, r_t is ~ 1.10 AU, while for $M_* = 6 M_\odot$ the corresponding value of r_t is ~ 1.40 AU (i.e., MS stars with larger masses are disrupted at larger distances).

A comparison of equations (2) and (3) reveals that for MS binaries we always have $r_{bt} > r_t$ (for contact binaries instead it is possible to disrupt a star before ejection occurs). Our numerical simulations demonstrate that for large binary separations where $r_{\text{per}} < r_{bt}$, the two stars remain bound to each other up to distances $\sim r_{bt}/2$. This can be understood if the dynamical crossing time of the binary at r_{bt} is of the order of the time scale of tidal breakup of the binary. Furthermore even at later times, after the binary is broken apart, both stars remain close to the original Keplerian orbit of the binary around the SMBH until reaching distances $\sim r_{\text{per}}$. We will come back to this point below.

Using equations (1) and (3) we can roughly estimate the lowest value of v_{in} that avoids tidal disruption of the individual stars. The condition $r_{\text{per}} > r_t$ yields

$$v_{\text{in}} \geq v_1^c \approx \left[\frac{2GM_\bullet}{(d^2/r_t + d)}\right]^{1/2}. \quad (4)$$

For $d = 0.01(0.1)\text{pc}$, this critical velocity is $v_1^c = 44(4.0)\text{ km s}^{-1}$ for $M_* = 3 M_\odot$ and $50(4.5)\text{ km s}^{-1}$ for $M_* = 6 M_\odot$. When PN corrections are included the orbits are no longer Keplerian and the periastron distance can be found by including relativistic terms in the expression for the potential (Soffel 1989):

$$V(r) = -\frac{GM_\bullet M_b}{r} + \frac{L^2}{2M_b r^2} - \frac{GM_\bullet L^2}{c^2 M_b r^3}, \quad (5)$$

where L is the binary angular momentum and c the speed of light. For a given initial velocity, the net relativistic effect consists of a decrease of r_{per} , yielding a higher limit for the initial velocity than for the Newtonian case. This value, in the case $d = 0.01\text{pc}$, is $v_1^c \sim 47$ and 53 km s^{-1} for $M_* = 3$ and $6 M_\odot$ respectively. For $v_{\text{in}} < v_1^c$ stars would be tidally disrupted.

We can derive an expression for the maximum initial velocity that should still be able to produce a HVS. The minimum condition is that the binary itself is broken apart. Together with equation (2), this gives

$$v_{\text{in}} \leq v_2^c \approx \left[\frac{2GM_\bullet}{(d^2/r_{bt} + d)}\right]^{1/2}. \quad (6)$$

Very few HVSs are likely to be ejected at $v_{\text{in}} > v_2^c$.

In this approximate model, HVSs are produced for $v_1^c < v_{\text{in}} < v_2^c$. Between these limits, one member of a binary may be captured by the SMBH and begin to orbit it at large eccentricity, while the other star is ejected with a velocity v_{ej} that is larger than the escape velocity from the Galaxy. An approximate expression for v_{ej} was obtained by Hills (1988) and Yu & Tremaine (2003):

$$v_{\text{ej}} \approx 1770 \left(\frac{a_0}{0.1\text{AU}}\right)^{-1/2} \left(\frac{M_b}{2M_\odot}\right)^{1/3} \left(\frac{M_\bullet}{3.5 \times 10^6 M_\odot}\right)^{1/6} f_{\text{R}} \text{ km s}^{-1} \quad (7)$$

with f_{R} a function of the dimensionless closest approach parameter $D = (r_{\text{per}}/a_0)[2 M_\bullet/10^6 M_b]^{-1/3}$. An expression for f_{R} was derived by Bromley et al. (2006):

$$f_{\text{R}} = 0.774 + (0.0204 + [-6.23 \times 10^{-4} + \{7.62 \times 10^{-6} + (-4.24 \times 10^{-8} + 8.62 \times 10^{-11} D)D\}D]D), \quad (8)$$

which reproduces the spectrum of ejection velocities for binaries initially unbound relative to the SMBH. For bound orbits, the ejection speeds will typically be smaller, unless very large apoapses are adopted.

4. TIDAL CAPTURES

We first devised a set of simulations to determine the rate at which stars are captured by the SMBH. Here, ‘‘capture’’ means that a star passes either inside the stellar tidal disruption radius r_t , or inside the innermost stable circular orbit (ISCO) at $3R_S$, $R_S \equiv 2GM_\bullet/c^2$; $R_{\text{ISCO}} \approx 0.25$ AU for $M_\bullet = 4 \times 10^6 M_\odot$. Naively, one expects that passage of the binary within either radius would result in both stars being captured. In fact, due to the finite size of the binary, it is possible for one star to be destroyed and the other to escape as a HVS.

We performed ~ 36000 integrations with equal mass $M_* = 3 M_\odot$ binaries, $a_0 = 0.05$ or 0.2 AU and $d = 0.01\text{pc}$,

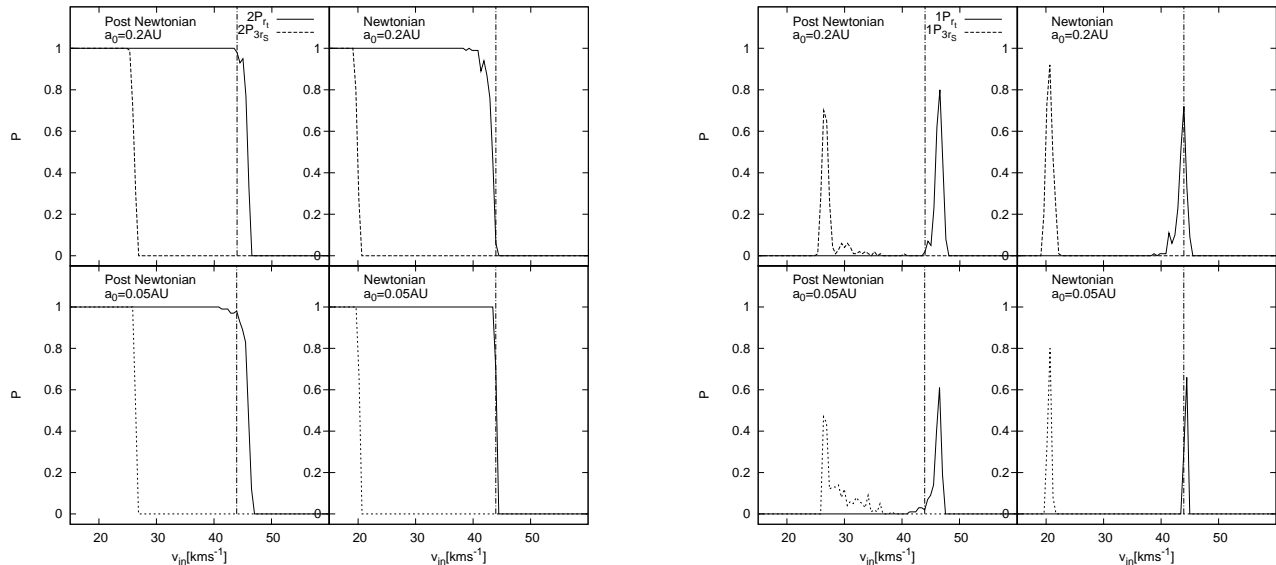


FIG. 1.— Probability that both stars (2P in the left panels) or only one star (1P in the right panels) of the binary fall within the tidal disruption radius r_t (solid lines) and the SMBH ISCO $3R_S$ (dashed lines) as a function of the initial velocity v_{in} . The vertical dot-dashed line represents the value of v_1^c .

choosing random orientations and initial tangential velocities in the range $4 \text{ km s}^{-1} \leq v_{\text{in}} \leq 85 \text{ km s}^{-1}$. For each of the two binary separations, we considered both Newtonian and PN cases. Stars were treated as point masses, and we recorded all instances when a star fell inside $3R_S$ or r_t . Given the possibility that only one of the two stars is captured during a close passage to the SMBH, it is important to include initial conditions with $r_{\text{per}} \lesssim r_t$ (or equivalently $v_{\text{in}} < v_1^c$).

Figure 1 shows the probability that one or both stars will pass inside $3R_S$ and/or r_t as a function of the initial velocity v_{in} . As a rule, passage of one star inside r_t or $3R_S$ implies that both stars are captured.

The probability that both stars are tidally disrupted rises essentially to one at $v_{\text{in}} \lesssim v_1^c \approx 44 \text{ km s}^{-1}$ in the classical case, and at a slightly higher velocity in the relativistic case.

The relativistic shift is well known: for a Keplerian orbit with $r_{\text{per}} \sim 1 \text{ AU}$, the difference in the relativistic periaapsis with respect to the Newtonian value is $\sim 0.12 \text{ AU}$, attributable to the attractive third term that appears in the relativistic potential in equation (5). Thus, when the binary has $v_{\text{in}} < 50 \text{ km s}^{-1}$, both stars are likely to be tidally disrupted by the SMBH.

Ginsburg & Loeb (2006) noted that the typical impact parameter that leads to the break-up of the binary by the black hole, is much larger than r_t , the tidal disruption radius for a single star. On this basis, they ignored stellar tidal disruptions. Our initial conditions are essentially the same as theirs; but as shown in Figure 1, these initial conditions would result in stellar tidal disruption for a large fraction of the orbits, contrary to the assumption of Ginsburg & Loeb. In their subsequent paper, Ginsburg & Loeb (2007) assumed $v_{\text{in}} < 25 \text{ km s}^{-1}$, which *always* leads to stellar disruption. Our study demonstrates that the relevant distance in the problem is the orbital periaapsis of the center of mass of the binary (equation 1), which is also the distance of the closest

approach of the stars to the SMBH. Indeed, for a wide range of initial velocities, the stars penetrate deeply the SMBH’s potential well. For $v_{\text{in}} \gtrsim 45 \text{ km s}^{-1}$ tidal disruption is avoided but tidal perturbations of the SMBH would still be expected to have a significant influence on the subsequent evolution of the stars.

Figure 1 also indicates that it is possible for only one star to be captured. In our calculations this mechanism does not produce a significant number of HVSSs since this occurs for a narrow range of initial velocities: $v_{\text{in}} \approx v_1^c$ in the classical case, and $v_{\text{in}} \gtrsim v_1^c$ in the relativistic case. Between these cases we found that for wider binaries ($a_0 = 0.2 \text{ AU}$) the non-disrupted star is typically still on a bound orbit around the SMBH while for tighter binaries ($a_0 = 0.05 \text{ AU}$) the ejection probability is around $\sim 80\%$ and the mean ejection velocity is $\sim 3000 \text{ km s}^{-1}$.

If r_{per} is slightly larger than r_t , the binary is usually disrupted at the first encounter with the SMBH. However we found a small fraction of orbits for which the binary survived for longer times. In our simulations, unbinding of the binary ($E_b \approx 0$) occurs approximately at 2 AU for $a_0 \approx 0.05 \text{ AU}$ and at $\sim 10 \text{ AU}$ for $a_0 \approx 0.2 \text{ AU}$. In the subsequent evolution the separation between the stars does not change appreciably until the periaapsis passage. After this point, the stars can either separate or become bound to each other again, continuing to orbit the SMBH as a binary. When this occurs, the minimum separation between the stars can become very small at later times.

An example of the latter situation is illustrated in Figure 2, which shows the evolution of the separation between the stars, as well as the orbit of the binary with respect to the SMBH, for an initial separation $a_0 \sim 0.05 \text{ AU}$ and initial velocity $v_{\text{in}} = 51 \text{ km s}^{-1}$. After the first encounter with the SMBH, where the internal binary eccentricity suddenly changes, the periaapsis separation between the stars is $\sim 0.035 \text{ AU}$ while the apoapsis separation is $\sim 0.08 \text{ AU}$. After the second encounter, the stars orbit each other on an elliptical orbit with peria-

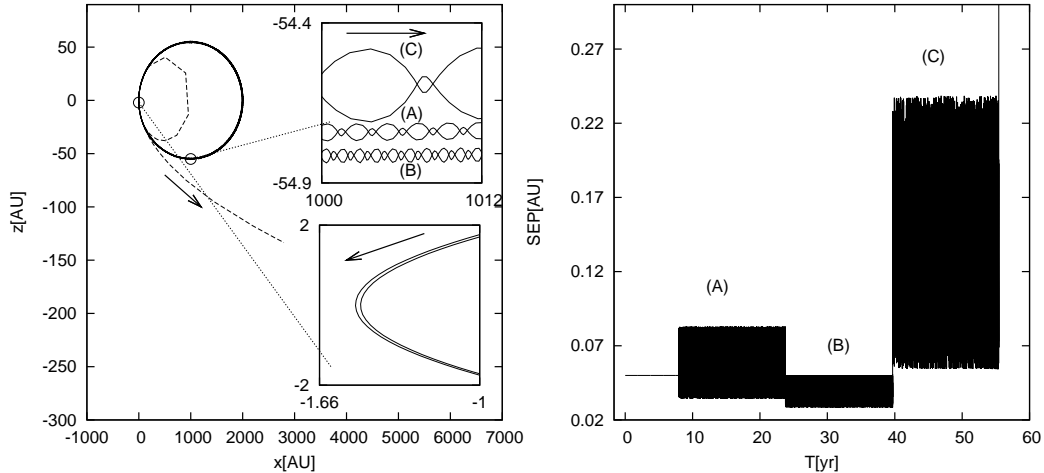


FIG. 2.— Example of an orbit whose periastron separation from the SMBH is $r_{\text{per}} \gtrsim r_t$. The binary is initially located at $x = 2000\text{AU}$ (0.01pc) with a purely tangential initial velocity of $v_z = 51\text{km s}^{-1}$. The stellar masses are $M_* = 3M_\odot$ with initial binary separation $a_0 = 0.05\text{AU}$. The left panel shows the orbit of the stars. The binary makes three revolutions around the SMBH before it is disrupted, after this point the individual stellar orbits are given by dashed lines. The upper inset panel schematically displays the different internal binary orbits during the first (A), second (B), and final loop (C). The lower inset panel shows the stars’ orbits with respect to the SMBH during the first encounter. Note that the x and z -axes have very different scales. The right panel displays the change of the separation between the stars with time. The upper and lower limits of each “block” represent apoapsis and periapsis of the internal binary orbit respectively.

sis separation $\sim 0.028\text{AU}$. The third encounter with the massive object results in a very eccentric orbit. Finally, after four encounters with the SMBH the binary is disrupted and the two stars begin to orbit the SMBH on two different high eccentricity orbits.

The previous arguments suggest that the eventual shrinkage of the orbit after the encounter with the SMBH can easily trigger mass transfer and, in extreme cases, a coalescence between the stars. The merger remnant would orbit the SMBH on a highly eccentric orbit. In the case displayed in Figure 2, the minimum separation between the stars is small enough to allow mass transfer after the second passage close to the SMBH. The Roche limit corresponding to the onset of mass transfer in binary systems of equal-mass stars would be $\sim 2.8R_*$ while the dynamical instability limit in the case of co-rotating equal-mass MS stars is located around $\sim 2.4R_*$ (Rasio & Shapiro 1992, 1995); for the case of eccentric binaries the radius of the Roche lobe is similar to that of circular binaries when calculated at periastron (Regös et al. 2005). We also stress that this scenario would hold for higher values of r_{per} , in which case it would not be restricted to small periastron separations, as will be shown below.

From this first set of integrations we deduce that cases in which only a single star is captured are relatively rare, and occur when $r_{\text{per}} \approx r_t$. Stars ejected from these orbits are expected to contribute weakly to the population of HVSs. This conclusion should hold in general when different values of d and M_* are chosen.

5. EJECTION OF HVS

For the remainder of this paper, we focus on cases where $r_{\text{per}} > r_t$. This allows us to neglect possible tidal effects on stars that would require a hydrodynamic treatment.

The tidal disruption of binaries by SgrA* is generally

TABLE 1
INITIAL PARAMETERS.

$a_0[\text{AU}]$	$M_*[M_\odot]$	$d[\text{pc}]$	Gravity
0.2	3	0.01	post-Newtonian and Newtonian
0.2	6	0.01	post-Newtonian and Newtonian
0.05	3	0.01	post-Newtonian and Newtonian
0.05	6	0.01	post-Newtonian and Newtonian
0.2	3	0.1	post-Newtonian
0.2	6	0.1	post-Newtonian
0.05	3	0.1	post-Newtonian
0.05	6	0.1	post-Newtonian

accepted to be the main source of HVSs (stars ejected with $v > 1000\text{km s}^{-1}$) in our galaxy. The maximum velocity that can be achieved with the classical binary supernova scenario (Blaauw 1961) is $\lesssim 300\text{km s}^{-1}$ for $3M_\odot$ stars. Interactions with a massive compact object seem necessary in order to explain the extreme velocities of HVSs.

In this section we explore this mechanism by integrating a set of ~ 10000 orbits featuring binary stars closely interacting with a SMBH. Two different stellar masses were considered: $M_* = 3M_\odot$ and $6M_\odot$. The runs were performed for initial velocities that correspond to periastron distances between r_t and $6r_{\text{bt}}$. In all the simulations the final integration time was fixed to 60 orbital periods of the initial binary orbit around the SMBH. For the adopted periastron distances, this integration time is long enough for the perturbations induced by the SMBH on the internal binary’s orbit to grow dramatically. Table 1 summarizes the initial parameters we chose for the integrations.

Because the binary is initially bound to the SMBH, no HVS is produced when two stars merge (i.e., if the relative velocity is lower than the escape velocity from the stellar surface after a collision). On the other hand, if the stars collide without merging the ejection of a single star is still possible. Hence, in the following, we assume that

TABLE 2
EJECTION PROBABILITIES FOR THE POST-NEWTONIAN (NEWTONIAN) RUNS DESCRIBED IN TABLE 1 FOR CASES WHERE $r_{\text{per}} < r_{\text{bt}}$.

a_0 [AU]	M_* [M_\odot]	d [pc]	Escape with $v_{\text{ej}} > 800 \text{ km s}^{-1}$	Escape with $v_{\text{ej}} > 1000 \text{ km s}^{-1}$	Escape with $v_{\text{ej}} > 1400 \text{ km s}^{-1}$	Escape SMBH
0.2	3	0.01	11.0(9.57)	9.71 (7.35)	6.60 (7.02)	28.2 (24.3)
0.2	6	0.01	55.5(56.3)	53.5 (49.7)	27.7 (27.5)	57.3 (60.7)
0.05	3	0.01	68.6(62.0)	66.7 (62.0)	65.6 (62.0)	72.0 (62.0)
0.05	6	0.01	54.2(66.0)	52.5 (65.1)	52.5 (65.1)	65.5 (66.3)
0.2	3	0.1	80.0	74.5	55.5	89.1
0.2	6	0.1	80.9	79.1	71.8	85.5
0.05	3	0.1	69.3	69.3	69.3	71.6
0.05	6	0.1	44.3	44.3	44.3	44.3

a HVS ejection is possible even after the stars collide, unless the final product is a merger.

5.1. Unbound population

Figure 3 displays the average asymptotic ejection velocity of the stars unbound from the central object, as well as a comparison with the approximate model described by equations (4), (6) and (7). Our results are in fair agreement with the predicted model, at least for $d = 0.1\text{pc}$. When the apoapsis of the initial orbit is reduced to $d = 0.01\text{pc}$ and $a_0 = 0.2\text{AU}$, the ejection speed of the unbound stars can be a factor of 2 smaller than the typical values found for initially unbound stars. For $a_0 = 0.05\text{AU}$, on the other hand, the results are in good agreement with the model. The larger discrepancy in the case of wider binaries with respect to the theoretical model (i.e., unbound orbits) is due to their larger value of r_{bt} . Since the ejection velocity depends strongly on the Keplerian velocity of the binary when its components start to separate, the contribution of the binary orbital energy to v_{ej} will be more important when the disruption occurs at larger distances from the SMBH. Another source of the observed discrepancy is due to the artificial truncation done at v_{ej}^c , beyond which a number of unbound stars are still produced which represent the tail of the distribution with the lowest values of v_{ej} . These cases are mainly due to binaries which are broken apart after few orbits around the central object. At each encounter the internal eccentricity of the binary changes, and there is a new chance for the stars to be separated and for a member to be ejected.

To demonstrate the orbital evolution during an integration, Figure 4 shows the change of the internal binary eccentricity e_b as a function of the distance to the SMBH for several representative cases with different initial velocities in both PN and Newtonian gravity. The eccentricity was evaluated from the specific angular momentum and binding energy of the binary: $e = \sqrt{1 + 2EL^2/(GM_b)^2}$. The initial separations, stellar masses, and apoapses were given respectively by $a_0 = 0.05\text{AU}$, $M_* = 3M_\odot$ and $d = 0.01\text{pc}$. The eccentricity behaves similarly for different initial conditions, increasing suddenly at $\sim r_{\text{bt}}$, though in some cases the orbits may do several passages within r_{bt} while maintaining a negative internal binary energy. When the binary has a small periapsis, several transitions between $e_b > 1$ (unbound) and < 1 (bound) are possible.

Results from our runs whose orbits have periapses within the binary tidal disruption radius (i.e., $r_{\text{per}} < r_{\text{bt}}$) are described in Table 2. In general, we find for wider binaries with $a_0 = 0.2\text{AU}$, lighter binaries with $M_* = 3M_\odot$

are less likely to produce HVSs capable of escaping the galaxy than heavier binaries with $M_* = 6M_\odot$, though they can produce a significant population of stars bound to the galaxy but unbound from the central SMBH. For tighter binaries with $a_0 = 0.05\text{AU}$ the situation is reversed, and lighter binaries are more likely to eject HVSs from the galaxy. For these tighter binaries, there are very few ejections of stars that unbind from the SMBH but remain bound to the galaxy, regardless of the stellar mass.

A comparison between the velocity distributions of the ejected stars in the Newtonian and PN cases reveals that relativistic effects have a slight influence on the mean properties of the sample. In particular for $a_0 = 0.05\text{AU}$ and $d = 0.01\text{pc}$ the mean ejection speed is larger when the relativistic corrections are included. For larger separations, instead, this effect is absent and the simulations show similar results. However, we were not able to identify a clear systematic effect due to the PN corrections in the properties of the ejected stars.

5.2. The Bound Population

Each star ejected during a binary-SMBH encounter is associated with a captured companion that loses energy in the process and becomes more tightly bound to the SMBH on a high eccentricity ($e \gtrsim 0.9$) orbit. Bound stars are also produced after the tidal break up of a binary if neither star is ejected. The orbital parameters of the bound stars will be strongly correlated with the amount of energy carried away by the companion. For an initially unbound orbit the apoapsis distance of the bound star is approximately

$$a \sim \frac{GM_\bullet}{v_{\text{ej}}^2}, \quad (9)$$

and the corresponding orbital period is

$$P \sim \frac{GM_\bullet}{v_{\text{ej}}^3}. \quad (10)$$

The mean value of the semimajor axis A (with respect to the massive body) for three-body exchanges with equal-mass binaries can be expressed as (Hills 1991)

$$\langle A \rangle \approx 0.56 \left(\frac{M_\bullet}{M_b} \right)^{2/3} a_0. \quad (11)$$

Bound stars can also be produced when the binary components merge. A coalescence remnant will not be able to escape the SMBH gravitational potential if the initial binary is bound to the SMBH unless significant mass loss occurs during coalescence.

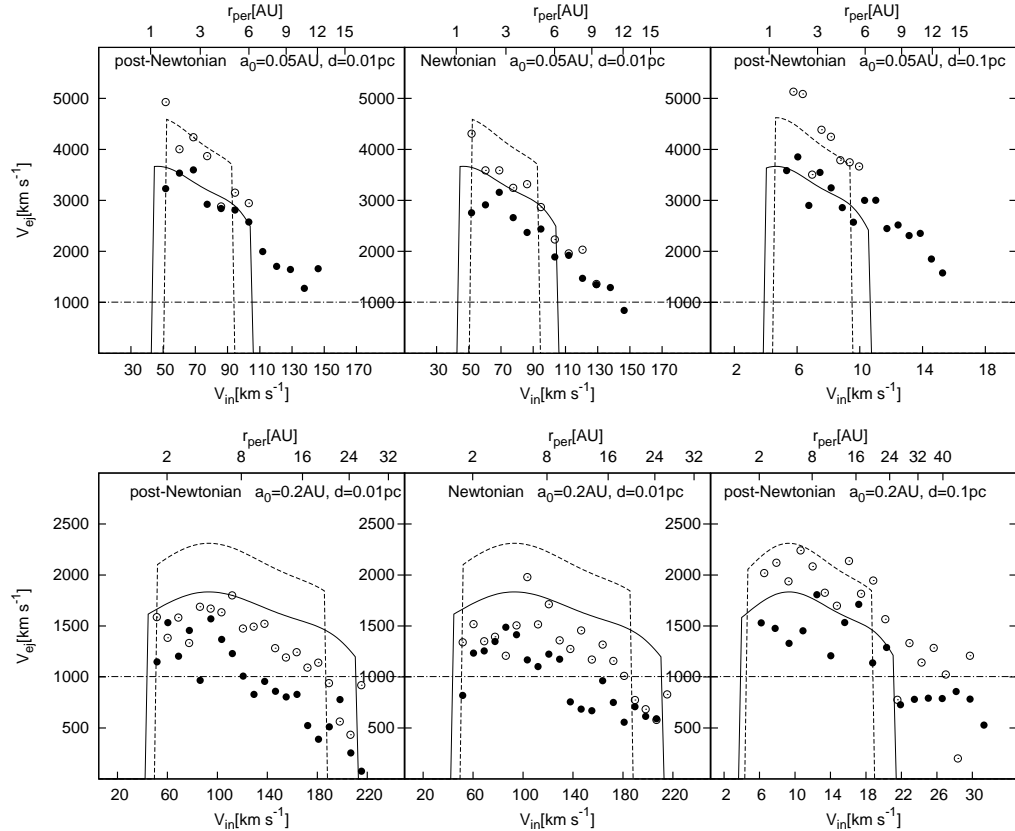


FIG. 3.— Average ejection velocity of the stars unbound to the SMBH for stellar masses $3 M_\odot$ (filled circles) and $6 M_\odot$ (open circles). The model described in §3 is superposed using dashed lines for $6 M_\odot$ and solid lines for $3 M_\odot$. The horizontal dot-dashed line shows the approximate escape velocity from the Milky Way ($\sim 1000 \text{ km s}^{-1}$).

Figure 5 shows the dependence of the average final eccentricity of bound stars on v_{in} . A decrease in v_{in} (and thus an increase in the eccentricity of the initial orbit) results in a larger final eccentricity for the bound star, while larger stellar masses and initial binary separations decrease the eccentricity of the captured star’s orbit. Figure 6 displays the eccentricity instead as a function of the orbital period of the stars that remain bound to the SMBH at the end of our PN simulations (the Newtonian calculations look similar). If we neglect the bound stars produced by mergers, three different families can be identified:

- 1) Bound stars whose companion also orbits the SMBH (grey open circles in Figure 6);
- 2) Bound stars whose companion has been ejected by the SMBH but remains bound to the Galaxy (red triangles in the figure);
- 3) Bound stars whose companion is a HVS escaping the Galaxy (filled circles in the figure). The approximate escape velocity from the Galaxy was chosen to be 1000 km s^{-1} which corresponds to stars able to reach distances larger than $\sim 100 \text{ kpc}$ from the Galactic center (Kenyon et al. 2008).

Due to the dependence of the apoapsis distance on the ejection velocity (see equation 9) the three families occupy distinct regions on the $e - P$ plane. If more kinetic

energy is deposited into the ejected star, the apoapsis distance of the bound star is reduced. In the case of equal mass binaries, the range of possible periods for the three populations of bound stars are independent of the stellar mass and the binary separation.

On the other hand, in the case of unequal mass binaries with $q = M_b/2M_1$ the apoapsis distance of the bound star can be approximated by

$$a_1 \sim \frac{GM_\bullet}{v_{ej}^2} q, \quad (12)$$

where v_{ej} is given by equation 7 and for moderate mass ratios, the probability to be captured is almost independent by the stellar mass.

Figure 6 shows that the stars with the highest values of P and e have reached velocities close to the escape velocity from the SMBH. Their companions also orbit the SMBH, but with much shorter periods. The region $e = 0.92 - 0.95$, strongly populated for $a_0 = 0.2 \text{ AU}$ and $d = 0.01 \text{ pc}$, is occupied by stars that were initially part of binaries with the largest values of v_{in} . For $d = 0.1 \text{ pc}$ bound stars are mainly companions of ejected stars and the comparable region is empty.

Stars whose the companion is escaping the Galaxy have orbital periods $\lesssim 50 \text{ yr}$. Many cases with orbital periods $\lesssim 10 \text{ yr}$ are also observed.

Finally, we note that in PN gravity the periastron distances of bound stars are about 0.1 AU smaller than in

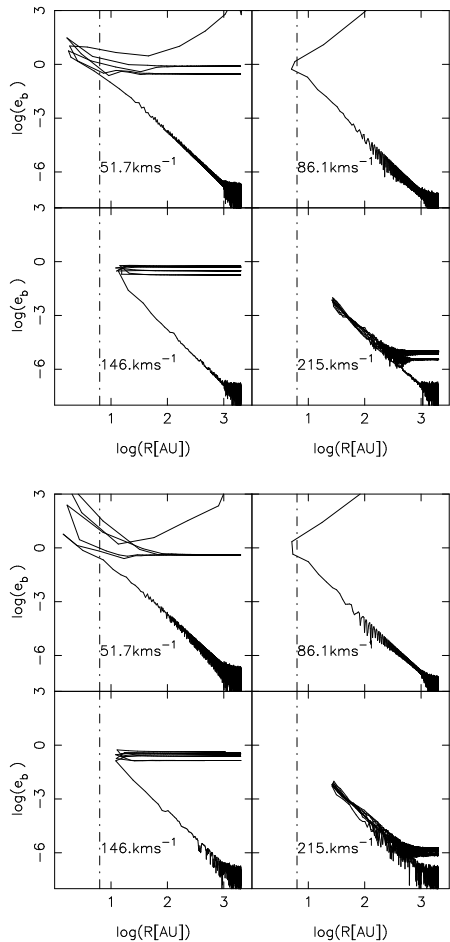


FIG. 4.— Internal binary eccentricity e_b as a function of the distance R to the SMBH for different initial velocities (displayed in the panels). The binaries have initial separation $a_0 = 0.05$ AU, stellar masses $3 M_\odot$ and the apoapsis is 0.01 pc. Top: Newtonian integrations. Bottom: PN integrations. The vertical dot-dashed line gives the value of r_{bt} . For small v_{in} , the binary approaches very near the SMBH and the encounter results in the tidal break-up of the binary. In some cases the binary can complete several orbits around the SMBH before its stellar components are finally separated, even though $r_{per} < r_{bt}$. Binaries with larger periapsis separations, or, equivalently, larger initial velocities, are likely to survive for a larger number of orbits. During each periapsis passage, gravitational interactions produce significant changes in the internal eccentricity of the binary.

the Newtonian regime.

6. COLLISIONS AND MERGERS

In this section, we study the evolution of binaries that are strongly perturbed during close passages to the SMBH, leading to stellar collisions and mergers. Stellar collisions due to either binary evolution or dynamical interactions are thought to be the main mechanism for the production of blue stragglers in star clusters (Collier et al. 1984; Benz & Hills 1987; Leonard 1989; Mateo et al. 1990). Similar processes may occur at the Galactic center, producing a population of “rejuvenated” stars. Genzel et al. (2003) proposed that the S-stars may be “super-blue stragglers” formed by collisions of lower mass stars and/or tidal heating. The apparent normality of their spectra (Eisenhauer et al. 2005) argues against rejuvenation (Figer 2008), but given the uncer-

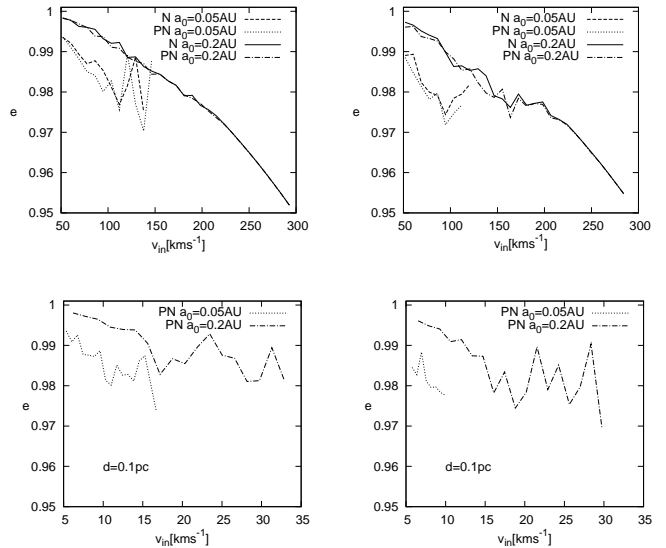


FIG. 5.— eccentricity versus the initial velocity v_{in} of the initial orbit with respect to SMBH, for the orbits of bound stars with masses $3 M_\odot$ (left panels) and $6 M_\odot$ (right panels). The eccentricity is average over initial binary orientation. Higher stellar masses and lower binary separations tend to reduce the orbital eccentricity of the captured stars.

tainties in the relaxation of merger products and the redistribution of angular momentum, it is difficult to draw firm conclusions as to their history.

It is possible that the S-stars are drawn from the young population observed in the stellar disk that extends inward to within 0.1 pc of the SMBH, but while the S-stars are primarily B dwarfs, the young stars in the disk are mainly luminous Wolf-Rayet and OB supergiants and giants (Paumard et al. 2001). This limits the connection between the two stellar populations, as O/W-R stars are typically more massive and shorter-lived than B types. Lückmann et al. (2008) proposed that binaries scattered from the stellar disk on highly eccentric bound orbits around the SMBH would be disrupted, ejecting one member as a HVS while leaving the other member bound. The inspiral of a cluster hosting an IMBH would generate stars on comparable orbits.

GL07 noted that the production of HVSs at the Galactic center could also result in collisions: the SMBH disrupts a binary, delivering an impulsive kick to one of the two stars at some direction with respect to the orbital plane, and under some circumstances the two stars will collide. We expect a dependence of the collision probability on the initial binary orientation (unless gravitational focusing dominates) and a correlation between the number of HVSs produced and the number of collisions. However, GL07 concluded that the frequency of mergers is so low that no star in the Galactic center is expected to have been produced by binary coalescence.

To investigate the rates of mergers and collisions using N -body techniques, we define the minimum impact parameter for a collision as $2R_*$, and the two stars are assumed to merge when their relative speed upon collision is lower than the escape velocity from their surfaces.

We find a much higher rate of coalescence than found by GL07, with most close collisions occurring only af-

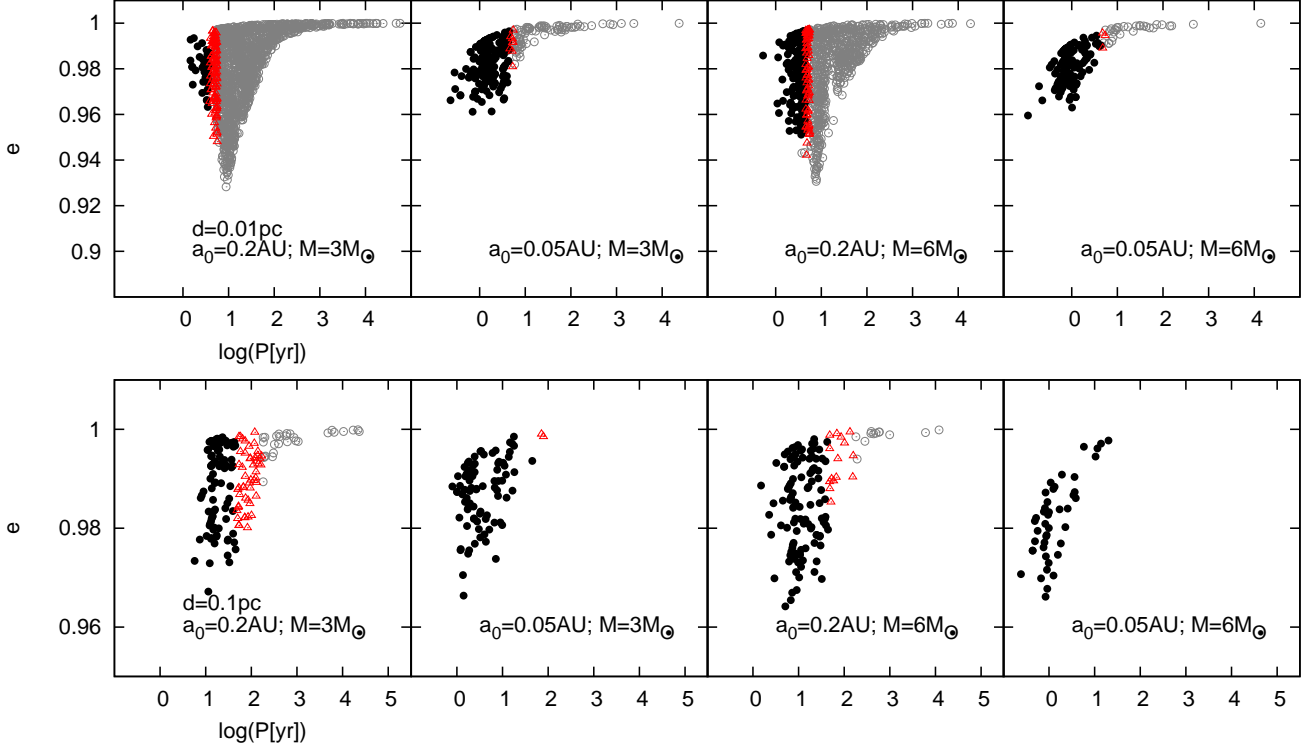


FIG. 6.— Eccentricity versus period for the orbits of the stars that remain bound to the SMBH at the end of the PN integrations. The grey open circles correspond to stars whose companion is also orbiting the SMBH but remains bound to the Galaxy but remains bound to the Galaxy are represented by red triangles, while stars whose companion escapes as a HVS are indicated by filled circles.

ter repeated encounters of the binary with the SMBH. The mechanism that leads to the majority of the close encounters in our integrations is Kozai oscillations.

6.1. Kozai oscillations

The perturbations on the inner binary's orbit caused by the gravitational interaction with the SMBH can result in periodic oscillations (Kozai cycles) of both the internal binary eccentricity e_b and the mutual inclination j (Kozai 1962). This occurs when the initial inclination j_{in} is sufficiently large and when the stars approach the SMBH at relatively large periapses ($\gtrsim r_{\text{bt}}$). More precisely, the perturbations from the SMBH on the inner binary must always be weak and j_{in} needs to satisfy the relation $i_c \leq j_{\text{in}} \leq 180^\circ - i_c$, where the critical angle i_c can be assumed to be $\sim 40^\circ$ in the case of initially circular binaries and Newtonian gravity. Kozai cycles can result in a reduction of the periapsis separation, allowing the inner bodies to collide. The period of the cycles can be written in terms of the masses of the three bodies, the eccentricity of the outer binary e and their semimajor axis as:

$$\begin{aligned} \tau &= \frac{P_{\text{out}}^2}{P_b} (1 - e^2)^{3/2} \left(\frac{M_b + M_\bullet}{M_\bullet} \right) K(e_b, \omega_b, j_{\text{in}}) \\ &\simeq \frac{P_{\text{out}}^2}{P_b} (1 - e^2)^{3/2} \end{aligned} \quad (13)$$

where P_b is the periods of the inner binary, P_{out} the external period, e_b and ω_b the inner binary eccentricity and argument of periapsis, and K is generally of order

unity (Ford et al. 2000). Writing

$$\begin{aligned} P_b &= 2\pi \left(\frac{a_0^3}{G M_b} \right)^{1/2} \\ &= 4.5 \times 10^{-3} \left[\left(\frac{a_0}{0.05 \text{AU}} \right)^3 \left(\frac{6M_\odot}{M_b} \right) \right]^{1/2} \text{yr} \end{aligned}$$

and

$$\begin{aligned} P_{\text{out}} &= 2\pi \left(\frac{[d/(1+e)]^3}{G M_\bullet} \right)^{1/2} \\ &= \frac{44.4}{(1+e)^{3/2}} \left[\left(\frac{d}{0.01 \text{pc}} \right)^3 \left(\frac{4 \times 10^6 M_\odot}{M_\bullet} \right) \right]^{1/2} \text{yr} \end{aligned}$$

the Kozai period becomes

$$\begin{aligned} \tau &\simeq \frac{2\pi}{\sqrt{G}} \frac{M_b^{1/2}}{M_\bullet} \left(\frac{d}{a_0^{1/2}} \right)^3 \frac{(1 - e^2)^{3/2}}{(1 + e)^3} \\ &= 4.4 \times 10^5 \left(\frac{a_0}{0.05 \text{AU}} \right)^{-3/2} \left(\frac{M_b}{6M_\odot} \right)^{1/2} \\ &\times \left(\frac{M_\bullet}{4 \times 10^6 M_\odot} \right)^{-1} \left(\frac{d}{0.01 \text{pc}} \right)^3 \frac{(1 - e^2)^{3/2}}{(1 + e)^3} \text{yr}. \end{aligned}$$

Thus, in our integrations, the Kozai period is between ~ 2 and ~ 120 times longer than the orbital period around the SMBH, and the full effect of the Kozai cycles is only felt after several revolutions.

TABLE 3
HVSs ($v_{ej} > 1000 \text{ km s}^{-1}$), COLLISION AND MERGER FREQUENCY(%) FOR RUNS WITH $r_{per} \leq 6r_{bt}$.

post-Newtonian (Newtonian); $d = 0.01\text{pc}$									
1 orbital period			5 orbital periods			60 orbital periods			
$a_0[\text{AU}], M_*[M_\odot]$	HVSs	Coll	Merg	HVSs	Coll	Merg	HVSs	Coll	Merg
0.2, 3	3.14 (3.00)	2.54(2.18)	1.50(2.15)	3.65 (3.25)	8.30 (9.10)	5.49 (5.29)	4.31 (3.26)	22.0 (20.5)	17.0(16.6)
0.2, 6	15.2 (15.4)	4.47(2.92)	3.01(2.62)	16.5 (16.7)	18.3 (12.5)	9.11 (9.59)	17.4 (16.8)	30.6 (30.6)	27.5(27.4)
0.05, 3	16.3 (16.8)	8.05(9.74)	5.97(5.45)	21.7 (18.2)	15.7 (23.4)	14.4 (20.6)	22.4 (21.0)	41.0(47.0)	40.1(43.8)
0.05, 6	15.6 (16.2)	13.8(16.2)	13.8(13.3)	15.9 (16.9)	24.3 (30.2)	23.9 (27.9)	20.8 (20.2)	47.5 (55.5)	47.1 (53.2)
post-Newtonian; $d = 0.1\text{pc}$									
1 orbital period			5 orbital periods			60 orbital periods			
$a_0[\text{AU}], M_*[M_\odot]$	HVSs	Coll	Merg	HVSs	Coll	Merg	HVSs	Coll	Merg
0.2, 3	29.0	1.66	1.00	30.0	5.00	3.60	30.0	18.6	17.1
0.2, 6	31.6	4.33	3.33	35.6	12.0	9.33	37.0	20.3	16.3
0.05, 3	25.0	8.33	8.05	27.1	21.7	21.0	28.0	30.3	29.6
0.05, 6	13.3	18.3	16.0	14.3	27.0	24.3	14.7	40.0	37.3

If the orbit is initially circular, the maximum eccentricity achieved during a Kozai cycle is

$$e_{b,\max} = [1 - (5/3) \cos^2 j_{\text{in}}]^{1/2}, \quad (14)$$

the amplitude of the oscillations depending only on the initial inclination of the inner orbit relative to the external perturber. The eccentricity of the outer binary remains roughly constant throughout the evolution, because its variation is caused by octupole interactions, which are weaker than the quadrupole interactions driving the oscillations of the inner binary's eccentricity (Takeda & Rasio 2005).

Kozai resonances can be suppressed by additional sources of apsidal precession such as tides and relativistic precession in the inner binary. The inclusion of PN effects between the two stars damps the oscillations of the inner orbital eccentricity, eventually causing a decrease in the number of observed collisions and mergers (Holman et al. 1997; Blaes et al. 2002).

6.2. Results

The results of our runs show, for what we believe to be the first time, that binary break-up is not a prerequisite for physical collisions, and that the collision probability increases strongly with time: increasing the simulation time (and thus the number of revolutions around the SMBH) results in a dramatic increase in the number of collisions. The first point is of particular relevance for binaries with high values of r_{per} , for which the SMBH more gradually reduces the internal binary angular momentum. This would allow the two stars to closely interact through mass transfer and eventually merge while they are still bound to each other. We note that the first encounter with separation $\leq 2R_*$ usually occurs just after the closest approach of the binary to the SMBH, when the orbital parameters suddenly change (see Figure 2). With regard to the second point: allowing the orbit to make only 2–3 extra revolutions around the SMBH increases the collision probability by up to three times with respect to shorter integrations (GL07). This is a consequence of the fact that the Kozai period is longer than the period of revolution around the SMBH.

Figure 7 gives four representative examples of how the inner binary parameters change when repetitive collisions

occur between the stars, with and without PN corrections. These cases are difficult to treat with an N -body approach, but we may safely conclude that the stars are likely to merge after a short time. When relativistic terms are included, the maximum value of the binary eccentricity reached in a Kozai cycle, $e_{b,\max}$, decreases. However, we found that the effect of relativistic precession on the likelihood of collisions and mergers observed in our simulations is weak.

In Table 3 we list the fraction of observed collisions, mergers, and HVS ejections after the first binary-SMBH encounter, after 5 orbital periods, and after 60 orbital periods. After the first encounter, most of the binaries with small periapsis are broken apart, depositing one star on a tight orbit around the SMBH while ejecting the companion as a HVS. The frequency of HVS ejection is nearly unchanged over time because the orbits with larger periapsis do not get close enough to the SMBH to eject a member. Such orbits, instead, suffer strong perturbations from the SMBH, altering the internal orbital parameters of the binary. The larger the periapsis, the larger the time required for the perturbations to become important, and the collision and merger frequency increase strongly with time. PN terms have important consequences only for initially small binary separations since the relativistic precession period is smallest for these systems. However, as shown in Table 3 the fraction of collisions is reduced by no more than 10% for $d = 0.01\text{pc}$, since for tight binaries even small eccentricities lead to close stellar encounters.

When the apoapsis is $d = 0.1\text{pc}$ the ratio between the timescale of relativistic precession in the binary and the period of the Kozai cycles becomes much smaller suppressing the Kozai resonance. Writing the timescale of relativistic precession as:

$$\begin{aligned} \dot{\omega} &= \frac{3G^{3/2} M_b^{3/2}}{a_0^{5/2} c^2 (1 - e_b^2)} \\ &= 4.9 \times 10^{-3} \left(\frac{M_b}{6M_\odot} \right)^{3/2} \left(\frac{a_0}{0.05\text{AU}} \right)^{-5/2} \text{yr}^{-1} \quad (15) \end{aligned}$$

with c the speed of light, the product $\dot{\omega}\tau$ of the initial configuration gives the relative strength of relativistic precession to that of the tidal field of the SMBH. For

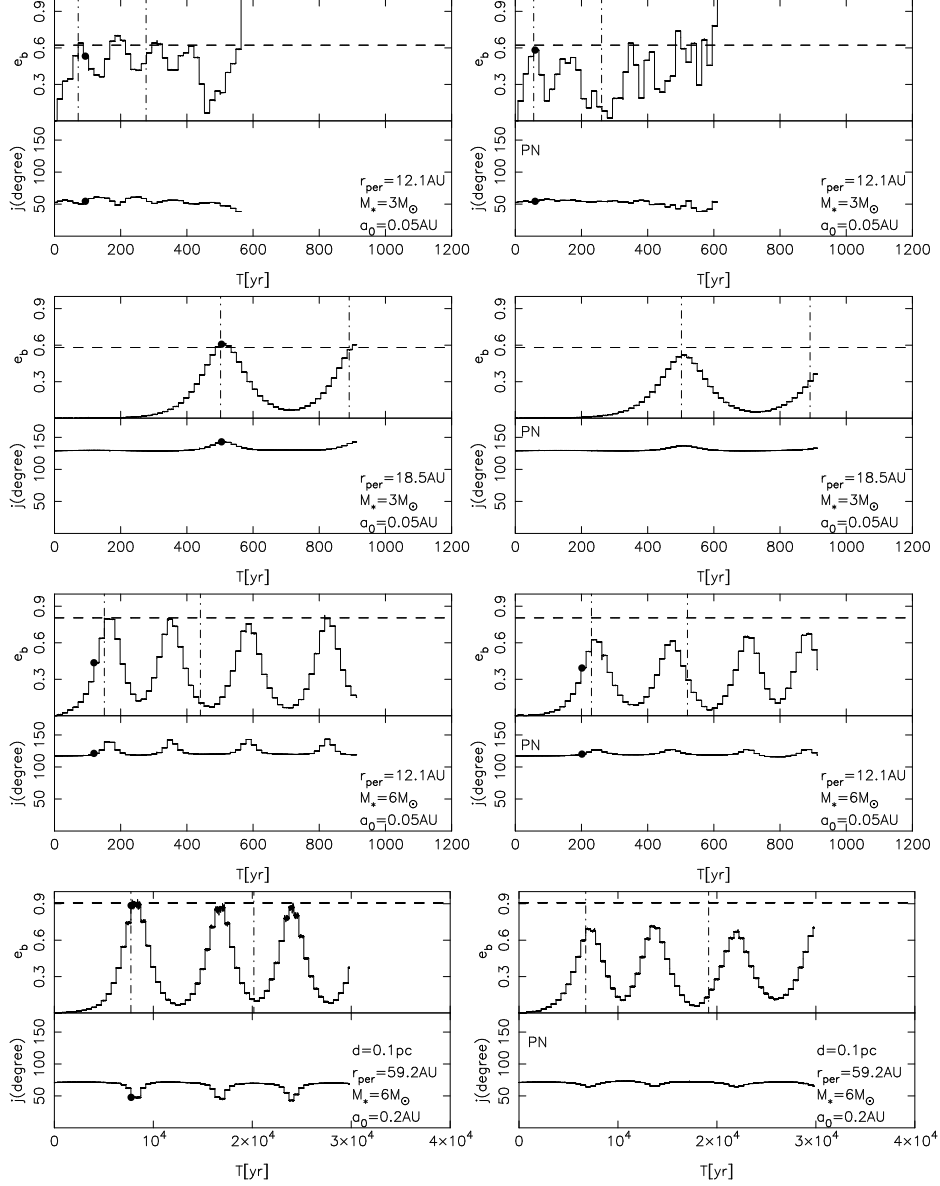


FIG. 7.— Evolution of the internal binary eccentricity and the mutual inclination j for different simulations in Newtonian (left panels) and PN (right panels) runs. In the cases shown, stars experience multiple collisions, and the time at which they finally merge is marked by a filled circle. For each periastron distance considered, the corresponding Newtonian and PN integrations were started from the same initial conditions. The top three rows have $d = 0.01$ pc and the bottom panels have $d = 0.1$ pc. The horizontal dashed lines mark the *classical* value $e_{b,\max}$ given in equation (14). The vertical dot-dashed lines give the Kozai timescale. When the periastron is sufficiently large the binary undergoes Kozai resonance, periodically changing both e_b and j . When PN terms are included the amplitude of the oscillations decreases, resulting in a larger survival time for the binary and a smaller probability for a collision. The bottom panels show the evolution for systems with $d = 0.1$ pc, for which the stars do not merge if PN corrections are included.

$M = 6M_\odot$ and $r_{\text{per}} \gtrsim 12\text{AU}$, this product can be as large as 10^2 and the Kozai cycles are completely suppressed (Fabrycky & Tremaine 2007). The ejection probability, instead, increases due to the larger eccentricity of the external orbit. The combination of these effects causes a smaller fraction of collisions/mergers respect to the number of HVSs.

Figure 8 displays the fraction of stellar mergers as a function of the periastron distance r_{per} , with most cases occurring for $r_{\text{per}} > r_{\text{bt}}$ where the Kozai mechanism becomes active. Figure 9 shows the cumulative fraction of stellar collisions, mergers and ejected HVSs in our PN integrations. Most of the HVSs are ejected during the

first periastron passage. Collisions and mergers, instead, typically occur later due to Kozai resonance, on a typical time scale $\sim \tau/2$, where τ is given by equation (13).

We note that strong mass transfer and/or mergers can lead to the formation of a rejuvenated star (Vanbeveren et al. 1998; Dray & Tout 2007).

The implications of these results for the actual rate of stellar mergers at the center of the Galaxy will depend on the dominant mechanism that drives binaries toward the SMBH. If binaries are scattered inward by “massive perturbers” (Perets et al. 2007), most of their orbits will be weakly bound or unbound with respect to the SMBH, with apoapses of order parsecs, and will only

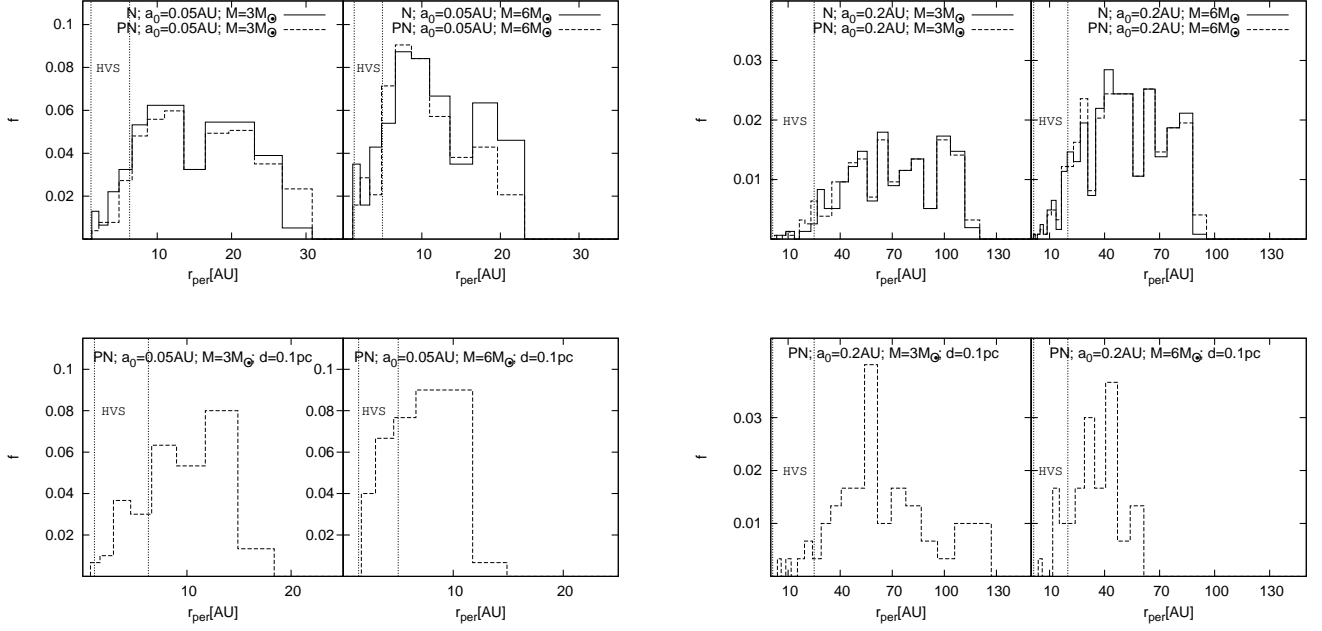


FIG. 8.— Fraction f of orbits leading to stellar mergers as a function of the periastron distance for PN and Newtonian simulations. The vertical dot-dashed lines bound the region where HVSs are produced.

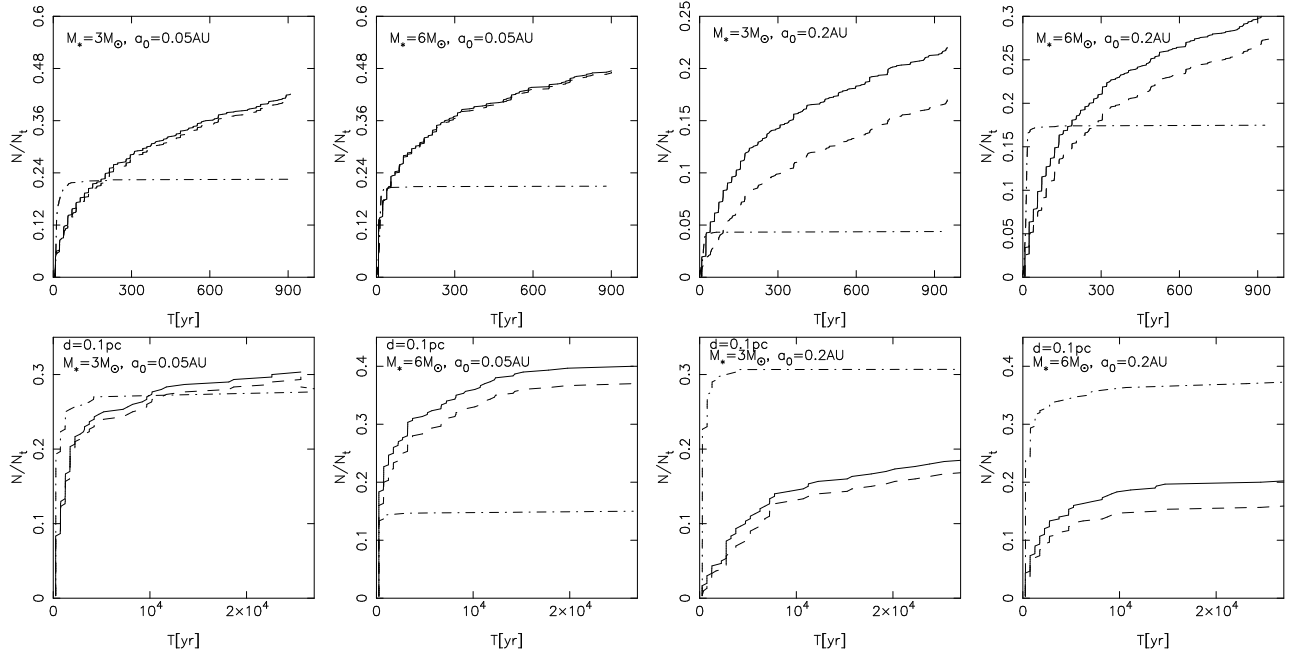


FIG. 9.— Cumulative fraction of stellar collisions (solid lines), mergers (dashed lines) and ejected HVSs (dot-dashed lines) in our PN integrations. Most of the HVSs are ejected during the first encounter with the SMBH; collisions and mergers, on the other hand, occur more frequently later after the inner binary's parameters have evolved due to the gravitational perturbations induced by the SMBH.

encounter the SMBH once before being scattered onto different orbits. Given the low probability which we find for collisions during the first encounter with the SMBH for $d = 0.1\text{pc}$, we do not expect a significant merger rate unless the binary population at the Galactic center is biased toward low values of a_0 . Moreover, if the binary is initially unbound, the merger product is likely to be ejected at low velocities and it will neither remain bound (unless substantial mass loss occurs) nor become a HVS. Alternatively, mergers in this scenario may result from disruption of triples that can leave binaries on bound orbits with small apoapse (Perets 2009b). Obtaining an explicit value for the merger rate would be difficult in this case given the large uncertainties about the population of multiple stellar systems in the Galactic center.

Alternatively, the binaries may form closer to the SMBH, perhaps in a disk, and migrate inward. In this case, the rate of collisions/mergers, as given in Table 3, would be comparable to the ejection rate of HVSs, i.e. $\sim 10^{-5}\text{yr}^{-1}$. However, given the strong dependence of the collision probability on the distance of closest approach to the SMBH, the merger rate will be strongly correlated with the periape distribution of the infalling binaries. The generation of massive new stars through binary-SMBH encounters in this scenario could possibly explain the presence of the stars that appear to be the youngest among the S-star group at the Galactic center (see also Perets (2009b) and Perets & Fabrycky (2009) for discussion on rejuvenating stars through Kozai-oscillation induced mergers).

In our simulations, the distribution of the semimajor axes and eccentricities of the captured stars are fixed by the initial distance d of the binary we adopt, and therefore is completely arbitrary. Nevertheless, as previously discussed, the apoapses found in our runs are consistent with those predicted assuming the binary progenitors of HVSs were scattered on eccentric orbits bound to the SMBH. The orbital eccentricities we find ($e > 0.95$), it should be noted, are larger than those observed for the S-stars at the Galactic center, which are consistent with a thermal distribution (i.e., $N(e) \propto e$). Perets et al. (2009) have shown how perturbations from a dense cluster of $10 M_\odot$ stellar black holes, expected to accumulate around the SMBH due to mass segregation (Hopman & Alexander 2006), tend to randomize orbits with high eccentricity in $\sim 20\text{Myr}$. Alternatively, if the binaries are transported to the center by the inspiral of a massive cluster containing an IMBH, interactions with the same IMBH will thermalize the eccentricities in $\sim 1\text{Myr}$ (Merritt et al. 2009). These processes of orbital randomization result also in the evolution of the periapsis distance r_{per} , but on a timescale much larger than that required for the binary systems to collide. We note, finally, that the presence of external forces on the inner binary as well as tidal friction between the stars could suppress the Kozai resonances reducing the number of stellar collisions.

6.3. Effect of the Initial Binary Orientation

Based on the results of our simulations, we find no strong dependence of the collision and/or merger probability during the first SMBH passage on the initial binary orientation. To quantify our results, we use the Rayleigh (dipole) statistic ζ_c (ζ_m) defined as the length of the re-

sultant of the unit vectors l_i , $i = 1, \dots, N$, where l_i is perpendicular to the initial internal orbital plane of the i^{th} binary system whose component stars collide (merge) during the integration and N is the number of collisions or mergers. Here the subscripts c and m refer to 'collision' and 'merger' respectively.

For an isotropic distribution $\zeta \sim \sqrt{N}$, while $\zeta \sim N$ if some preferential direction exists (Rayleigh 1919).

In order to test the agreement with an isotropic distribution we used a Monte Carlo approach: for each set of simulation parameters we generated a set of 1000 samples, each containing N randomly oriented orbits. Then, for the whole sample we computed the average of ζ and the corresponding standard deviation and we compared the resulting values with those obtained for the colliding/merging binaries.

Table 4 gives the estimated values of ζ after the first binary-SMBH encounter as well as the expected values for an isotropic distribution. Assuming a confidence interval of 90%, most of the values shown in Table 4 are consistent with an isotropic distribution.

We find values of ζ_m too large to be consistent with isotropy only for PN integrations where $a_0 = 0.05\text{AU}$ and $d = 0.01\text{pc}$, though for Newtonian integrations with the same apoapsis and $a_0 = 0.05\text{AU}$, the values of ζ_m are quite large as well, possibly indicating some degree of anisotropy. In Figure 10, we plot the spatial projection of the angular momentum eigenvectors for the inner binary, showing that when the angular momentum is aligned with the $+y$ -axis, the stars are unlikely to merge. These binaries are retrograde and their internal orbital plane coincides the orbital plane of the binary with respect to the SMBH. In all the other cases we conclude that the collision probability does not show any significant dependence on the initial binary orientation during the first encounter with the SMBH.

At later times stellar collisions are mainly produced by the Kozai mechanism which is active only for large initial inclinations j_{in} . This corresponds to a low probability of collisions for binaries with the angular momentum aligned with either the $\pm y$ -axis. For these cases our Rayleigh statistic results are still consistent with isotropy, but this is found to be an artifact attributable to the dipole nature of the Rayleigh statistic. A more careful analysis of the orbital distribution of binaries whose components merge at later times shows that, as expected, the population of colliding binaries is strongly biased toward large inclinations of the inner orbit with respect to the external orbital plane. An illustrative example is given in fig 11 which shows the projection of the internal angular momentum vectors for binaries with $a_0 = 0.2\text{AU}$ and $d = 0.01\text{pc}$ merging between 10 and 60 orbital periods. Even though the result of our statistical analysis in this case is consistent with isotropy, the distribution of the angular momenta is clearly anisotropic with most of the collisions occurring for large inclinations. The discrepancy is a consequence of the dipole nature of the Rayleigh statistic: the majority of the unit vectors l_i have a quasi-antialigned counterpart giving a net contribution close to zero.

7. SUMMARY AND DISCUSSION

We have carried out post-Newtonian numerical integrations of binary stars on highly elliptical orbits around

TABLE 4
 RALEIGH STATISTICS ζ_c AND ζ_m AND VALUES EXPECTED FOR AN ISOTROPIC DISTRIBUTION FOR COLLISIONS (EV_c) AND MERGERS(EV_m)
 AFTER THE FIRST BINARY-SMBH ENCOUNTER.

Post-Newtonian(Newtonian); d=0.01pc				
$a_0[AU], M_*[M_\odot]$	ζ_c/N	EV_c	ζ_m/N	EV_m
0.2, 3	0.33 (0.30)	0.18±0.15	0.25 (0.29)	0.23 ± 0.18
0.2, 6	0.19 (0.23)	0.17±0.14	0.21 (0.25)	0.20 ± 0.16
0.05, 3	0.20 (0.18)	0.12±0.10	0.26 (0.21)	0.13 ± 0.11
0.05, 6	0.16 (0.14)	0.10±0.08	0.21 (0.15)	0.11 ± 0.09
Post-Newtonian; d=0.1pc				
a_0, M_*	ζ_c/N	EV_c	ζ_m/N	EV_m
0.2, 3	0.45	0.38±0.26	0.46	0.43 ± 0.27
0.2, 6	0.14	0.17±0.14	0.30	0.30 ± 0.24
0.05, 3	0.28	0.20±0.16	0.33	0.20 ± 0.17
0.05, 6	0.14	0.14±0.11	0.16	0.15 ± 0.12

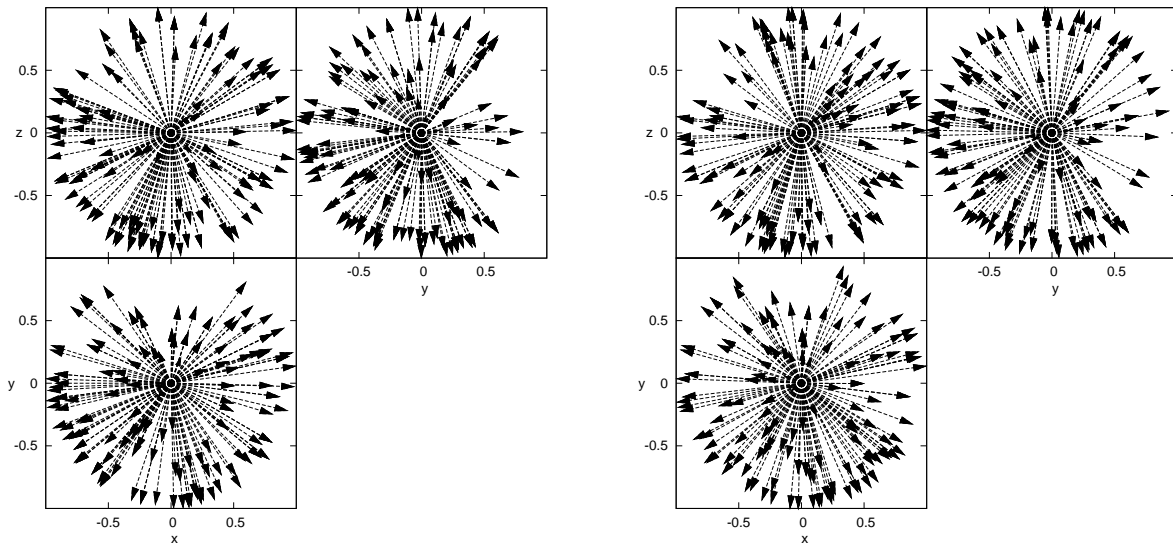


FIG. 10.— Projection of the angular momentum eigenvectors for binaries with $a_0 = 0.05$ AU and $d = 0.01$ pc merging during the first encounter with the SMBH for PN (left panels) and Newtonian (right panels) runs. A slight dependence of the merger likelihood on the initial binary orientation is observed, with a deficit apparent for initial orbits whose angular momentum is aligned with the $+y$ -axis. The deficit is less significant in the Newtonian integrations.

a supermassive black hole and classified the final fates of both stars. Our main conclusions can be summarized as follows:

1. If the binary orbit passes through the stellar tidal disruption radius r_t of the SMBH, both stars are likely to be disrupted during the initial passage, although there is a non-trivial chance that one star may remain outside the tidal disruption radius while the other passes within. We found that after the binary internal energy becomes positive the stellar orbits remain close to the initial trajectory of the disrupted progenitor. This demonstrates that HVSs can suffer strong tidal perturbations and mass loss before ejection.

2. Binaries with periaapses in the range $r_t < r_{\text{per}} < r_{\text{bt}}$ with $\sim r_{\text{bt}}$ the tidal breakup radius of the binary are the main hypervelocity star progenitors. In these cases

the (hypervelocity) ejection probability is typically larger than 50%, although the combination of wider separations ($a_0 = 0.2$ AU) and small apoapses ($d = 0.01$ pc) can result in probabilities less than 30%.

3. For tighter binaries (taken here to have separations of 0.05 AU), there is a strong inverse correlation between the periaapse distance of the binary and the HVS ejection velocity, while the dependence is present but weaker for wider binaries.

4. While many binaries perform several orbits around the SMBH before merging and/or colliding, the vast majority of HVSs were produced during the first passage by the SMBH. This is due to the strong dependence of HVS production on the periaapse distance of the binary orbit: binaries that get sufficiently close to the SMBH are broken apart, while those farther away will typically

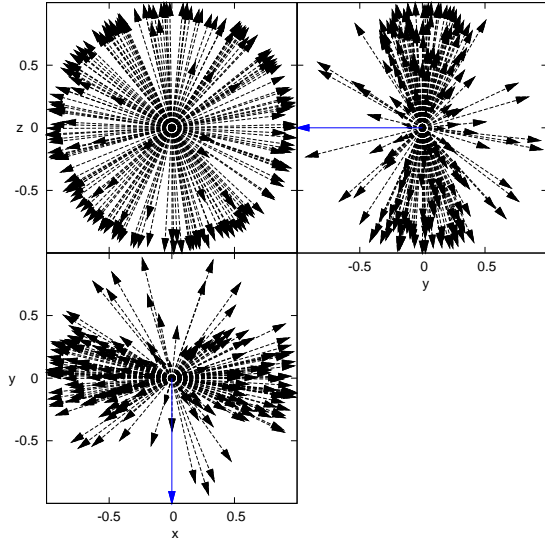


FIG. 11.— Projection of the angular momentum eigenvectors for binaries with $a_0 = 0.2$ AU and $d = 0.01$ pc merging between 10 and 60 orbital periods for Newtonian runs. This shows how the Kozai mechanism selects highly inclined orbits (the external orbital plane lies on the x - z plane and the direction of angular momentum corresponding to the external orbit is given by a blue continue arrow).

be unbound or collide.

5. The tidal break-up of equal-mass binaries by the SMBH results in a population of bound stars with periods and eccentricities defined mainly by the fate of the companion star (Fig. 6). Companions to escaping hypervelocity stars remain bound to the SMBH with orbital periods $P \lesssim 50$ yr, but also extremely short periods $P < 1$ yr are found. A much larger range of periods ($10^2 \lesssim P \lesssim 10^5$) is instead possible for stars whose companion is also left orbiting the SBH.

6. For sufficiently inclined orbits, the Kozai mechanism produces periodic oscillations of the inner binary eccentricity. This reduces the internal binary periastron allowing for close stellar encounters. We find that the probability for collisions between the components of

the binary increases with time, resulting in substantially larger numbers of mergers than in simulations that stop after the first passage.

7. When the external orbital period is large compared to the period of relativistic precession in the inner binary the PN corrections tend to suppress the oscillations reducing the probability of a collision which, however, remains high in our integrations. For initially bound orbits with $r_{\text{per}} < 6r_{\text{bt}}$ the probability that the two stars collide is similar (for $d = 0.1$ pc) or much larger (for $d = 0.01$ pc) than that of hypervelocity ejection.

Stars caught on highly eccentric orbits around the SMBH (with periastron $r_t < r < 2r_t$) can eventually spiral in as their orbital energy is converted into heat through tidal interactions during each periastron passage (e.g. Alexander & Morris 2003). Such stars would have orbital properties generally consistent with the S-star population, but N -body calculations cannot accurately predict the properties of the merger products. Instead, in a future work, we plan to study the evolution of binaries as they orbit the BH and collide or merge using a smoothed particle hydrodynamics (SPH) code, to determine the properties of the resulting stars, including their masses and angular momentum distributions. This should help to clarify whether they would be expected to possess normal spectra or features more commonly associated with blue stragglers.

Finally, our study provides concrete evidence that relativistic effects can have important consequences for the distribution of HVSs and the collision/merger probabilities of HVS progenitors.

We are extremely grateful to S. Mikkola who wrote the ARCHAIN algorithm and who generously assisted us in using it. We also thank T. Alexander, H. Perets, and H. Nakano for helpful conversations. J.A.F. was supported by NASA grants HST-AR-11763.01 and 08-ATFP08-0093. D. M. and A. G. were supported by NASA grant NNX07AH15G and by NSF grants AST-0807810 and AST-0821141.

REFERENCES

- Aarseth, S. J. 1999, *PASP*, 111, 1333
 Alexander, T. 2005, *Phys. Rep.*, 419, 65
 Alexander, T., & Morris, M. 2003, *ApJ*, 590, L28
 Benz, W., & Hills, J. G. 1987, *ApJ*, 323, 614
 Blaauw, A., 1961, *BAN*, 15, 265
 Blaes, O., Lee, M. H., & Socrates, A. 2002, *ApJ*, 578, 775
 Bromley, B. C., Kenyon, S. J., Geller, M. J., Barcikowski, E., Brown, W. R., & Kurtz, M. J. 2006, *ApJ*, 653, 1194
 Brown, W. R., Geller, M. J., Kenyon, S. J., & Kurtz, M. J. 2005, *ApJ*, 622, L33
 Brown, W. R., Geller, M. J., Kenyon, S. J., & Kurtz, M. J. 2006, *ApJ*, 647, 303
 Brown, W. R., Geller, M. J., Kenyon, S. J., Kurtz, M. J., & Bromley, B. C. 2007, *ApJ*, 671, 1708
 Brown, W. R., Geller, M. J., & Kenyon, S. J. 2009, *ApJ*, 690, 1639
 Collier, A. C., & Jenkins, C. R. 1984, *MNRAS*, 211, 391
 Dray, L. M., & Tout, C. A. 2007, *MNRAS*, 376, 61
 Duquennoy, A., & Mayor, M. 1991, *A&A*, 248, 485
 Eckart, A., & Genzel, R. 1997, *MNRAS*, 284, 576
 Eisenhauer, F. et al. 2005, *ApJ*, 628, 246
 Eggleton, P. P. 1983 *ApJ*, 268, 368
 Evans, C. R., & Kochanek, C. S. 1989 *ApJ*, 346, 13
 Faber, J. A., Rasio, F. A., & Willems, B. 2005 *Icar.*, 175, 248
 Fabrycky, D., & Tremaine, S. 2007, *ApJ*, 669, 1298
 Ferrarese, L., & Ford, H. 2005, *Space Science Reviews*, 116, 523
 Figer, D. F. 2008, *in Massive Stars: From PopIII and GRBs to the Milky Way (in press)*; preprint at <http://arxiv.org/abs/0803.1619>
 Ford, E. B., Kozinsky, B., & Rasio, F. A. 2000, *ApJ*, 535, 385
 Genzel, R., Eckart, A., Ott, T., & Eisenhauer, F. 1997, *MNRAS*, 291, 219
 Genzel, R., Schödel, R., Ott, T., Eisenhauer, F., Hofmann, R., & Lehnert, M. et al. 2003, *ApJ*, 594, 812
 Gerhard, O., 2001, *ApJ*, 546, L39
 Ghez, A. M., et al. 2008, *ApJ*, 689, 1044
 Gillessen, S., Eisenhauer, F., Trippe, S., Alexander, T., Genzel, R., Martins, F., & Ott, T. 2009, *ApJ*, 692, 1075
 Ginsburg, I., & Loeb, A. 2006 *MNRAS*, 368, 221
 Ginsburg, I., & Loeb, A. 2007 *MNRAS*, 376, 492
 Gould, A., & Quillen, A. C. 2003, *ApJ*, 592, 935

- Gualandris, A., Portegies Zwart, S., & Sipior, M. S., 2005, MNRAS, 363, 223
- Hansen, C. J., Kawaler, S. D., & Trimble, W. 2004, Stellar Interiors, Springer-Verlag New York, Inc.
- Hills, J. G. 1988, MNRAS, 368, 221
- Hills, J. G. 1991, AJ, 102, 704
- Holman, M., Touma, J., & Tremaine, S. 1997, Nature, 386, 254
- Hopman, C., & Alexander, T. 2006, ApJ, 645, L133
- Kenyon, S. J., Bromley, B. C., Geller, M. J., & Brown, W. R. 2008, ApJ, 680, 312
- Kozai, Y. 1962, AJ, 67, 591
- Leonard, P. J. T. 1989, AJ, 98, 217
- Löckmann, U., Baumgardt, H., & Kroupa, P. 2008, ApJ, 683, L151
- Luminet, J. P., & Carter, B. 1986, ApJS, 61, 219
- Madigan, A., Levin, Y., & Hopman, C. 2009, ApJ, 697, L44
- Merritt, D. 2006, Reports of Progress in Physics, 69, 2513
- Merritt, D., Gualandris, A., & Mikkola, S. 2009, ApJ, 693L, 35
- Mateo, M., Harris, H. C., Nemeč, J., & Olszewski, E. W. 1990, AJ, 100, 469
- Mikkola, S., & Aarseth, S. 2002, Celestial Mechanics and Dynamical Astronomy, 84, 343
- Mikkola, S., & Merritt, D. 2006, MNRAS, 372, 219
- Mikkola, S., & Merritt, D. 2008, AJ, 135, 2398
- Miller, M. C., Freitag, M., Hamilton, D. P., & Lauburg, V. M. 2005, ApJ, 631, 117
- Paczynski, H.B. 1971, ARA&A, 9, 183
- Paumard, T., Maillard, J. P., Morris, M., & Rigaut, F. 2001, A&A, 366, 466
- Perets, H. B., Hopman, C., & Alexander, T. 2007, ApJ, 656, 709
- Perets, H. B. 2009a, ApJ, 690, 795
- Perets, H. B. 2009b, ApJ, 698, 1330
- Perets, H. B., Gualandris, A., Kupa, G., Merritt, D., & Alexander, T. 2009, arXiv:0903.2912
- Perets, H. B., & Fabrycky, D. C. 2009, ApJ, 697, 1048
- Rayleigh, L. 1919, Phil. Mag., 37, 321
- Rasio, F. A., & Shapiro, S. L. 1992, ApJ, 401, 226
- Rasio, F. A., & Shapiro, S. L. 1995, ApJ, 438, 887
- Regös, E., Bailey, V. C., & Mardling, R. 2005, MNRAS, 358, 544
- Sesana, A., Haardt, F., & Madau, P. 2007, MNRAS, 379L, 45
- Sesana, A., Madau, P., & Haardt, F. 2009, MNRAS, 392, 31
- Soffel, M. H. 1989, Relativity in Astrometry, Celestial Mechanics and Geodesy (Springer-Verlag: Berlin)
- Takeda, G., & Rasio, F. A. 2005, ApJ, 627, 1001
- Vanbeveren, D., De Loore, C., & Van Rensbergen, W. 1998, A&A Rev, 9, 63
- Yu, Q., & Tremaine, S. 2003, ApJ, 599, 1129